[Global Biogeochemical Cycles]

Supporting information for

Controls on sinking velocities and mass fluxes of size-fractionated marine particles in recent U.S. GEOTRACES cruises

Yang Xiang[1,*], Phoebe J. Lam[1], Adrian Burd[2]

[1]Department of Ocean Sciences, University of California, Santa Cruz, CA 95064 USA
[2]Department of Marine Sciences, University of Georgia, Athens, GA 30602 USA

*Corresponding author: Yang Xiang, E: yaxiang@ucsc.edu, P: 1-831-212-5119
University of California Santa Cruz, 1156 High Street, Santa Cruz, CA 95064

Contents of this file:

Figures S1-S9
Table S1-S2

Additional supporting information:

Table S3. Size-fractionated mass flux and WSV in three cruises (uploaded separately)

Introduction

The supporting information mostly consists of two types of figures: depth profiles and section plots. Depth profiles are used to describe the difference in particle composition between different cruises. Parameters plotted in section plots include the mass-size spectra power q, derived parameters (WSV and mass flux) in the LSF and SSF, and sensitivity studies on the TOT mass flux. Supplemental tables contain information about sources and details of compiled datasets in the porosity-size relationship, size ranges used in the model, and derived mass flux and WSV in all three cruises.

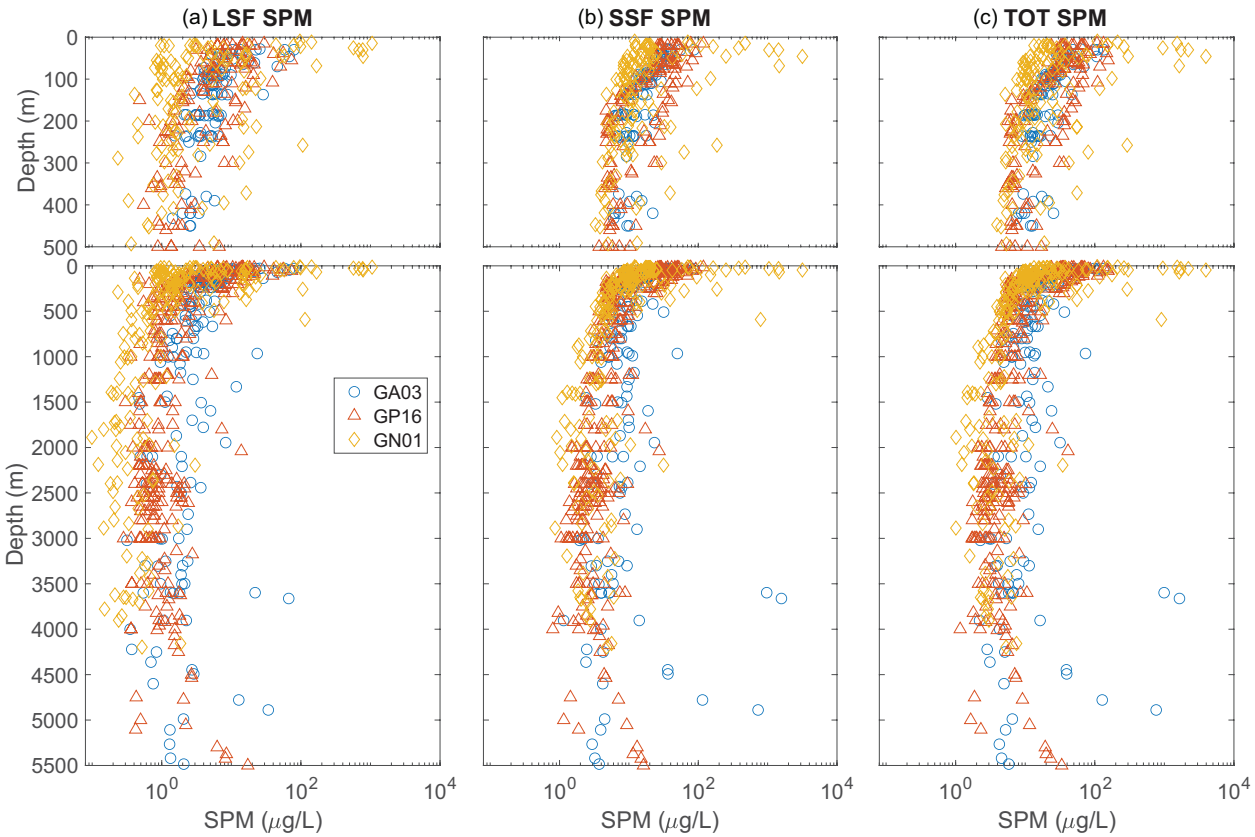

Figure S1. Depth profiles of size-fractionated SPM concentrations (unit: μg/L) in the upper 500 m (top panels) and the whole water column (bottom panels) in all three basins. (a): LSF (>51 μm); (b): SSF (1-51 μm); (c): TOT (>1 μm).

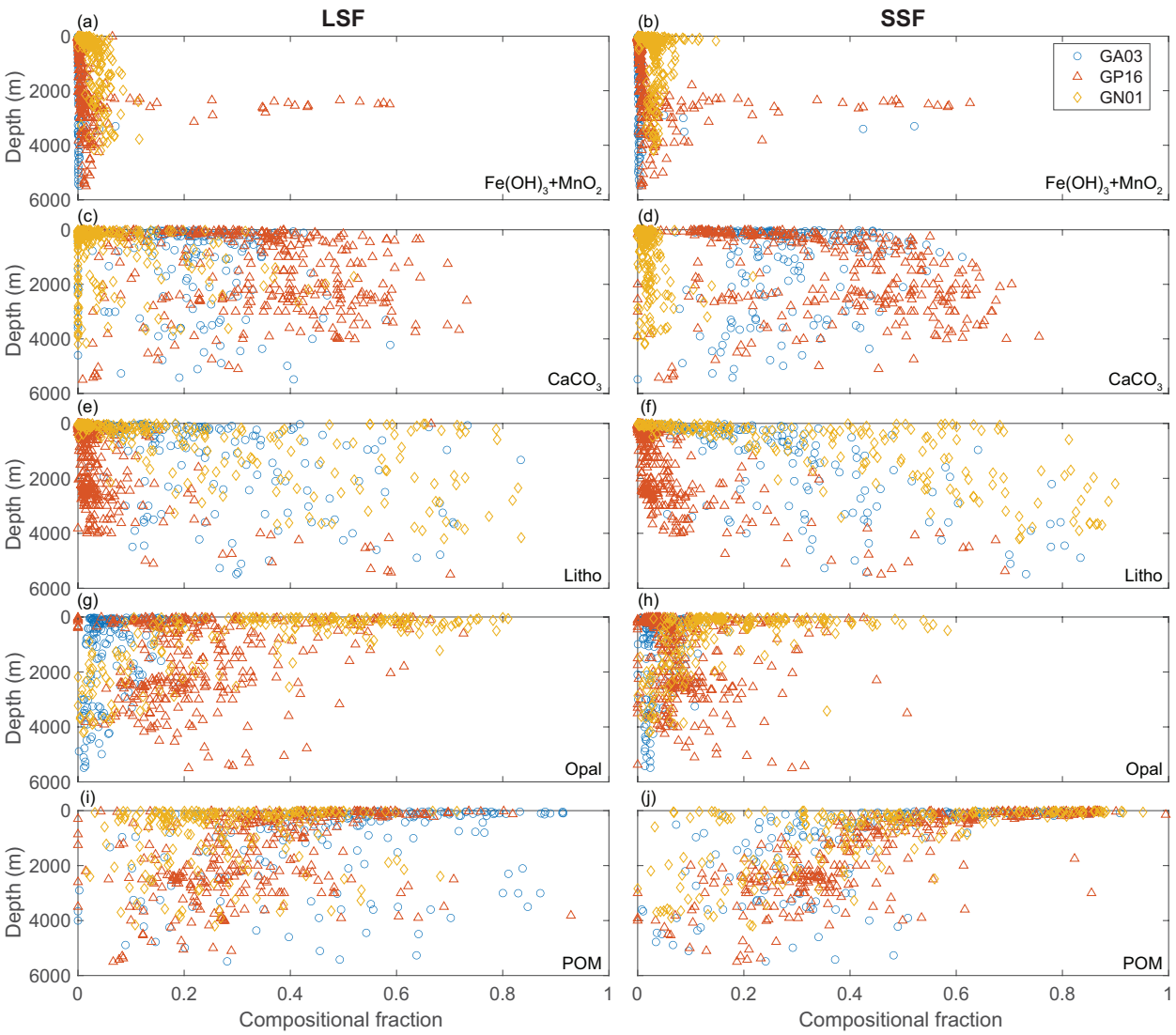

Figure S2. Depth profiles of size-fractionated compositional fractions in the LSF (left panels) and SSF (right panels) in all three basins. (a)-(b): the sum of fractions of iron and manganese (oxyhydr)oxides ($Fe(OH)_3$+MnO_2); (c)-(d): the fractions of calcium carbonate ($CaCO_3$); (e)-(f): the fractions of lithogenic materials (Litho); (g)-(h): the fraction of opal; (i)-(j): the fraction of particulate organic matter (POM).

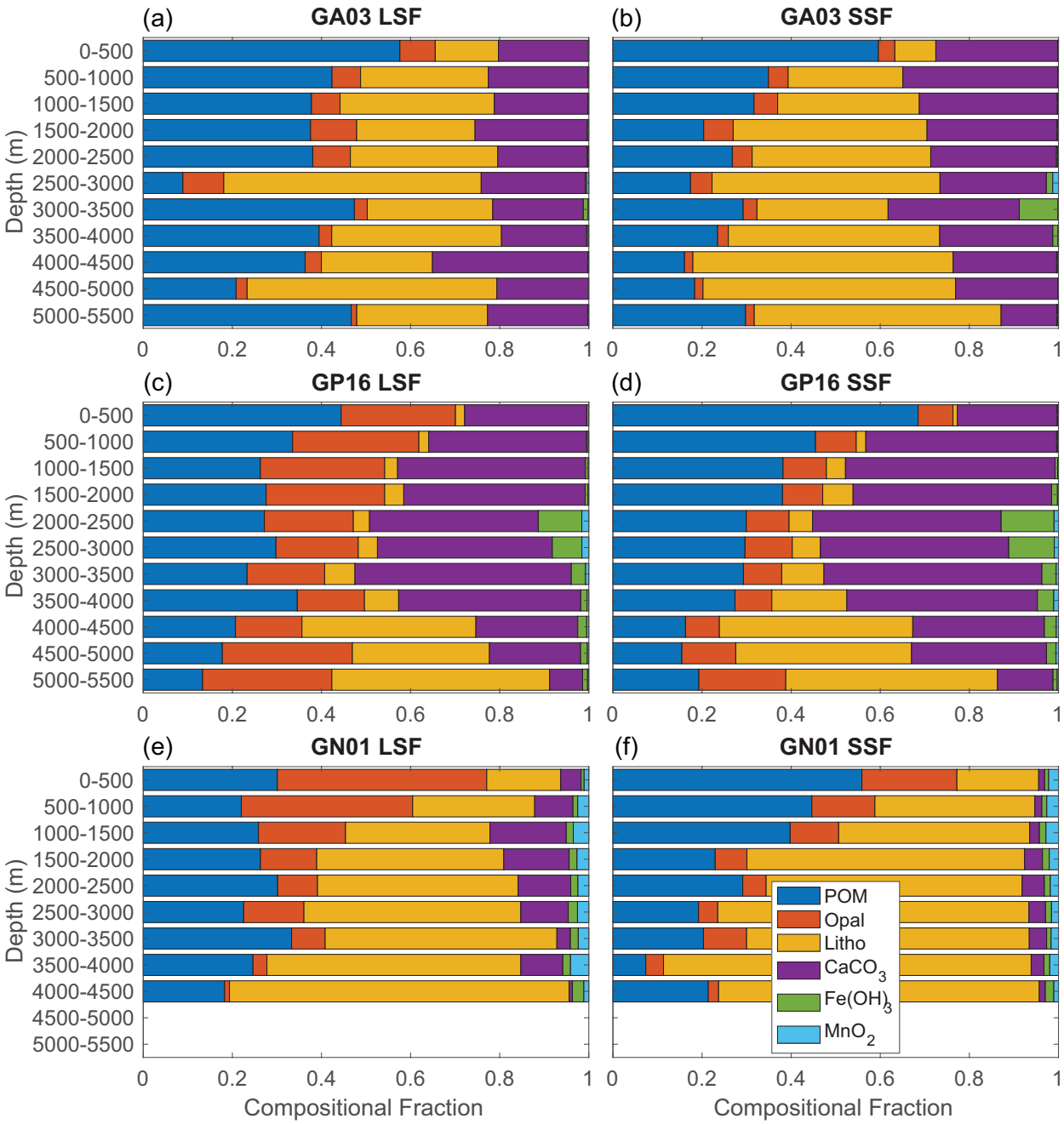

Figure S3. Stacked bar graphs of the change in size-fractionated compositional fractions in all cruises with depth. The left panels are the LSF and right panels are the SSF. Each 500 m depth bin shows the mean compositional fraction over the entire cruise. The blue is the compositional fraction of POM, orange is the fraction of opal, yellow is the fraction of lithogenic, purple is $CaCO_3$, green is Fe oxyhydroxides and light blue is Mn oxides. (a)-(b): GA03; (c)-(d): GP16; (e)-(f): GN01.

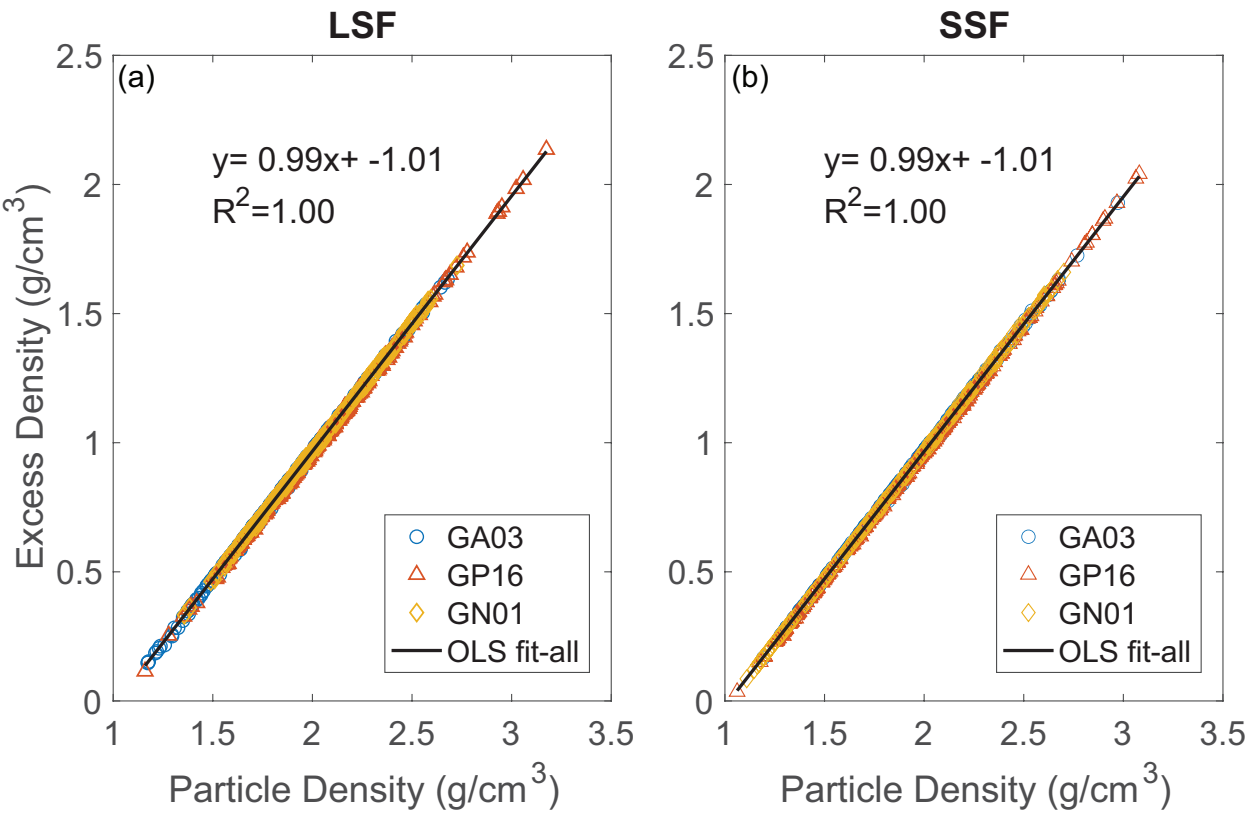

Figure S4. Size-fractionated particle density (unit: g/cm^3) vs. excess density (unit: g/cm^3) in three cruises. (a): LSF; (b): SSF. The ordinary least square (OLS) fit is used in the regression. Regression equations are displayed in each panel.

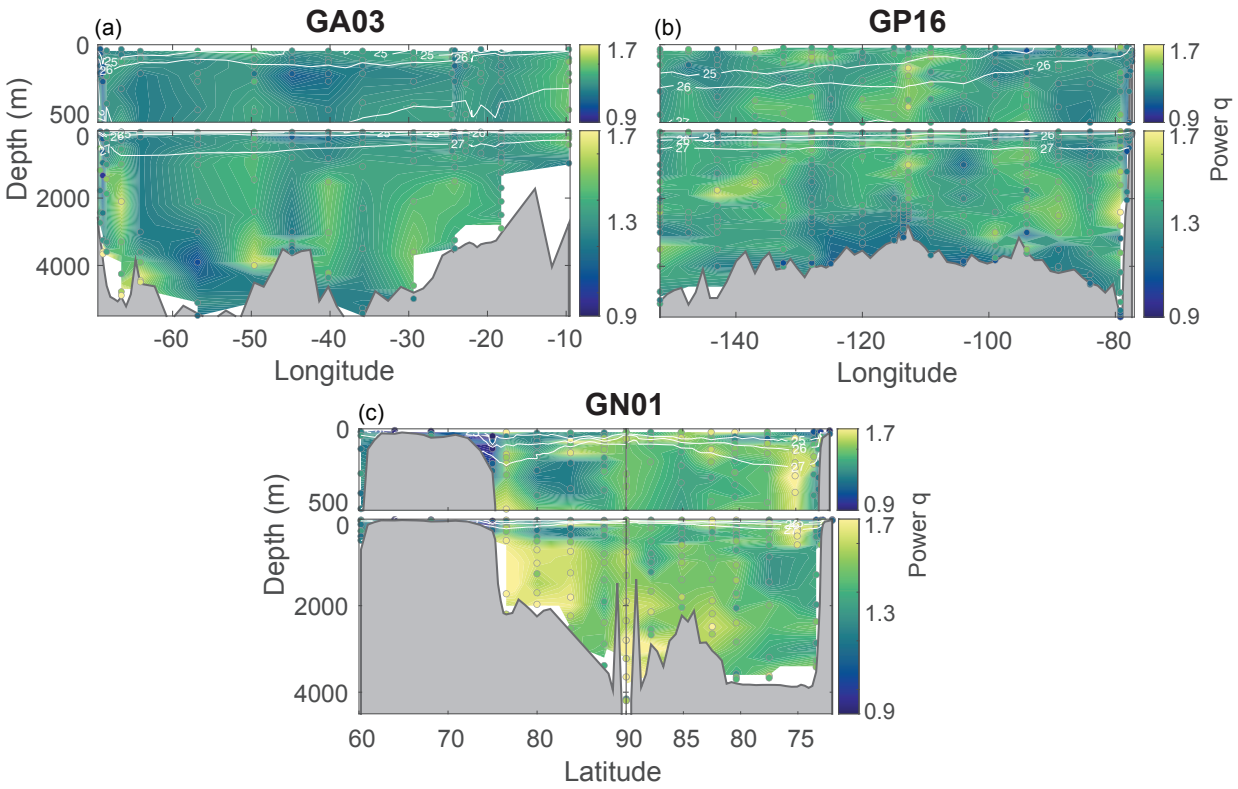

Figure S5. The power exponent q of the mass-size spectra in three cruises. (a): GA03; (b): GP16; (c): GN01. The top panels in each subplot show the upper 500 m, and the lower panels show the entire water column. Thick white contours are potential density anomaly of 25, 26 and 27 kg/m^3.

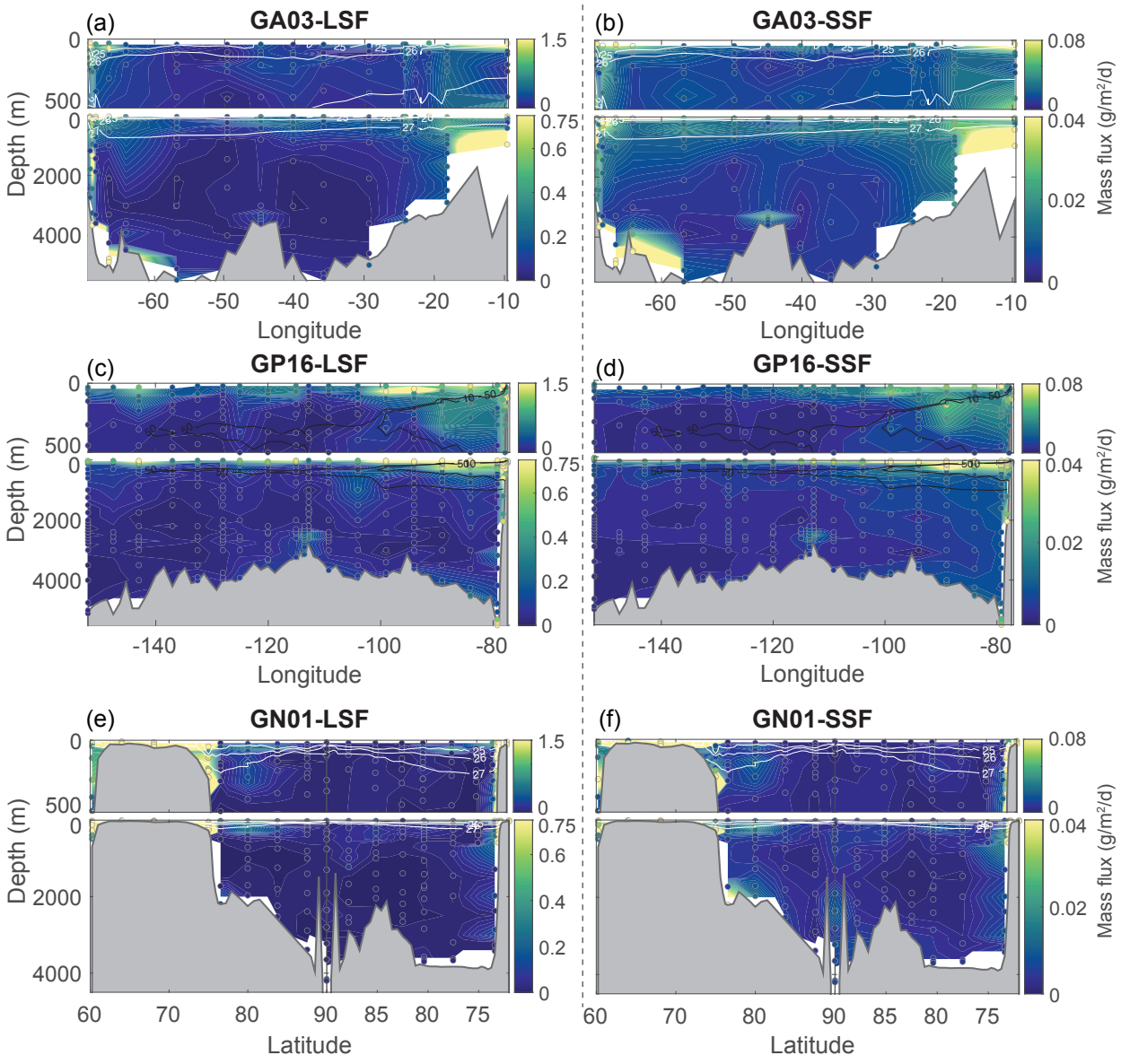

Figure S6. Derived mass flux (unit: g/m^2/d) in the LSF (left panels) and SSF (right panels) in three cruises. (a): GA03 LSF; (b): GA03 SSF; (c): GP16 LSF; (d): GP16 SSF; (e): GN01 LSF; (f): GN01 SSF. Thick white contours are potential density anomaly of 25, 26 and 27 kg/m^3, and thick black contours in the GP16 are dissolved oxygen concentrations of 10 and 50 μmol/kg. Note that color scales are the same for each size fractions in all cruises but are different between the LSF and SSF, and between the upper 500 m and the entire water column.

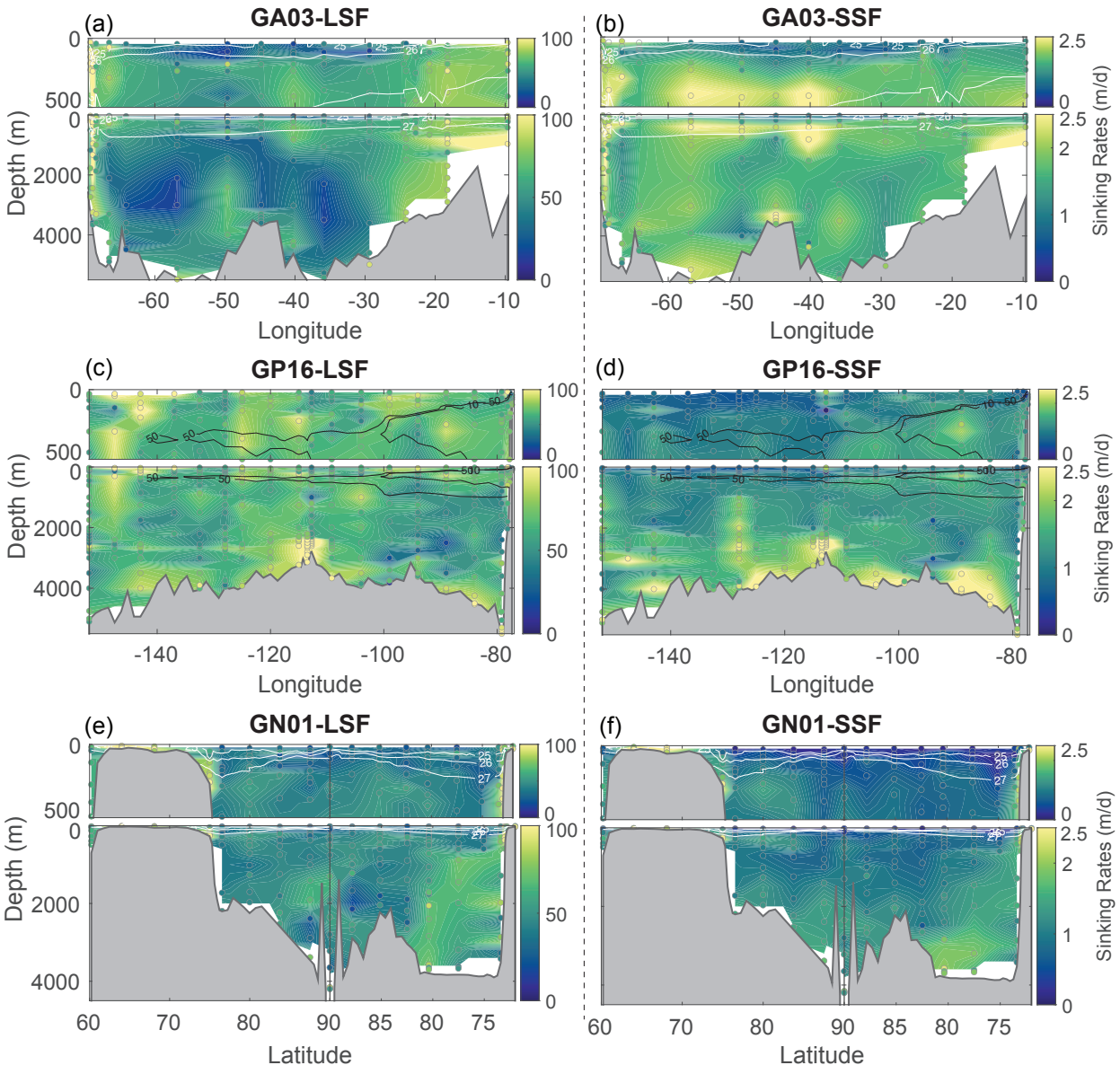

Figure S7. Derived mass-weighted average sinking velocity (unit: m/d) in the LSF (left panels) and SSF (right panels) in three cruises. (a): GA03 LSF; (b): GA03 SSF; (c): GP16 LSF; (d): GP16 SSF; (e) GN01 LSF; (f): GN01 SSF. Contours as for Figure S6.

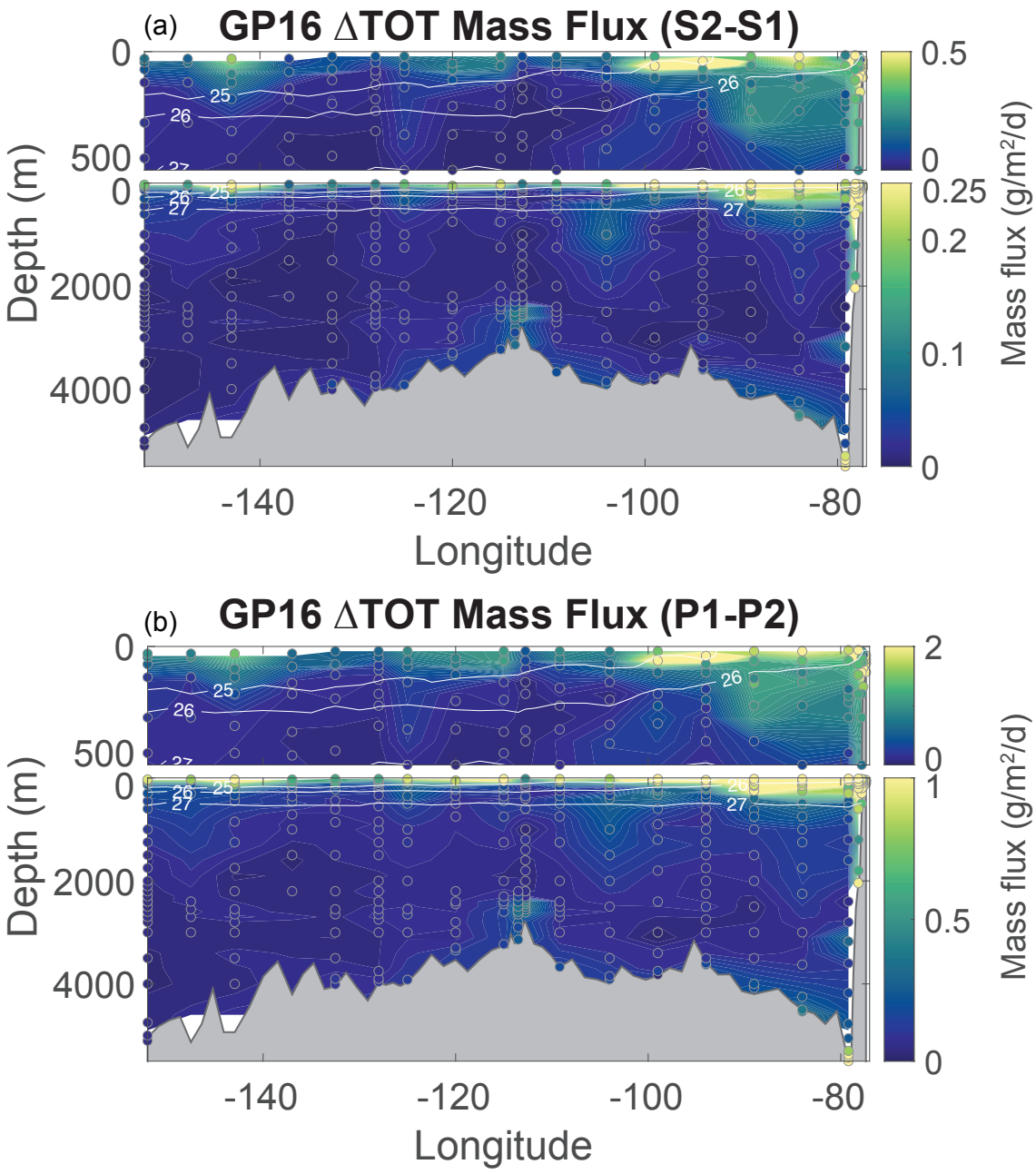

Figure S8. Sensitivity studies. (a) the absolute differences in TOT mass flux between two upper size limits in the LSF (S2-S1), S2 as 10 mm and S1 as 5 mm; (b) the absolute differences in TOT mass flux between two porosity-size relationships (P1-P2), where P1 is the relationship from Alldredge & Gotschalk (1988) and P2 is the newly compiled one in this study. Note that (a) and (b), together with their upper (upper 500 m) and lower (the whole water column) panels, all have different color bars.

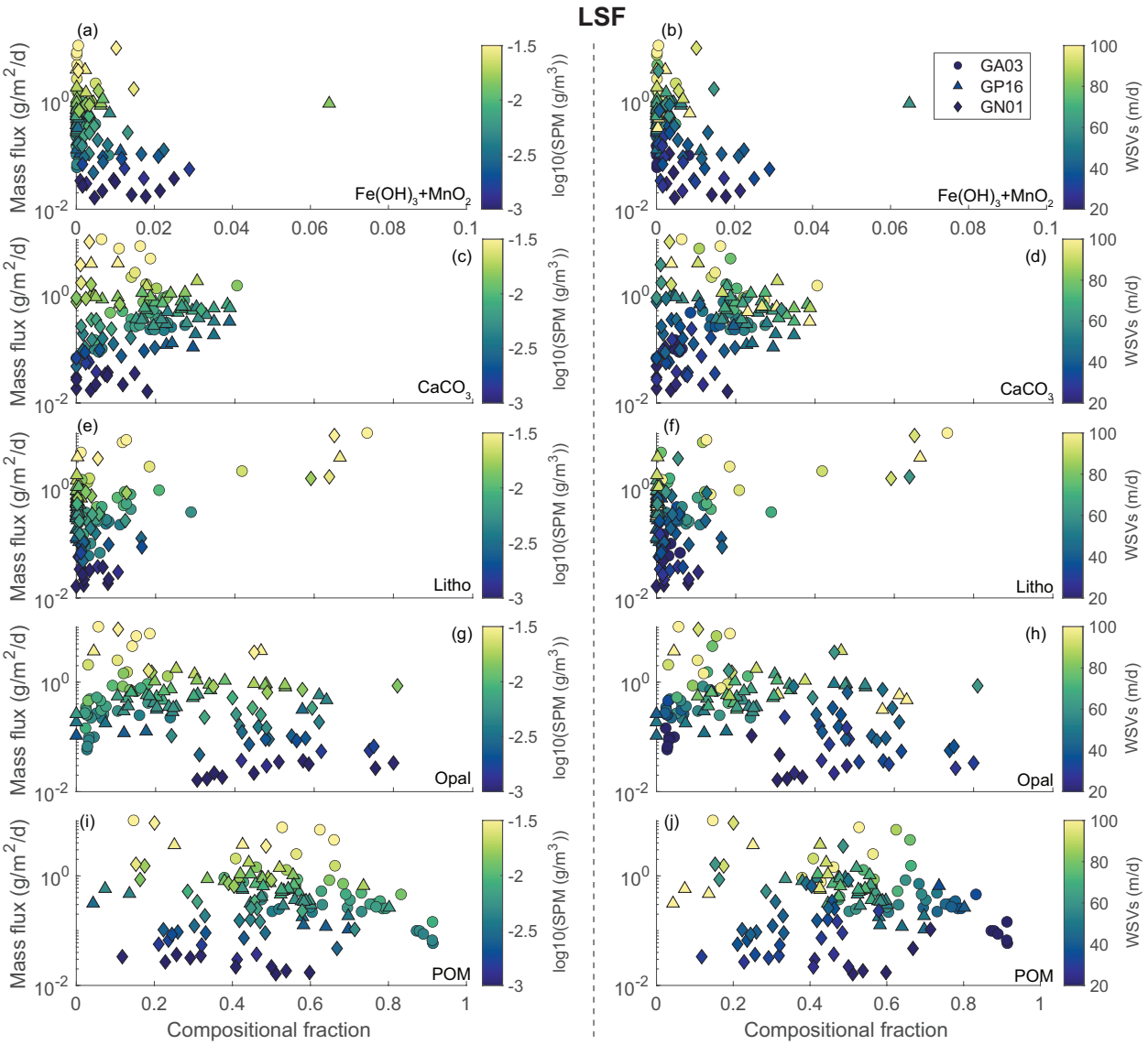

Figure S9. Scatter plots between LSF compositional fractions and LSF mass flux in the upper 100 m of all non-shelf stations (bottom depth>200 m). The color bars are log10(SPM) on the left, and mass-weighted average sinking velocity (WSVs) on the right. Note that the color bar for SPM is in log scale. The first row of plots (a-b) are the compositional fractions of $Fe(OH)_3$+MnO_2, the second row (c-d) the fractions of $CaCO_3$, the third row (e-f) the fractions of Litho, the fourth row (g-h) the fractions of Opal, and the fifth row (i-j) the fraction of POM. The fractions of $Fe(OH)_3$+MnO_2 have different X scales (0-0.1) than other compositional fractions (0-1).

Table S1. *Porosity-size Relationship Literature Compilation*

Sources	Size (Y/N)	Size error (Y/N)	Porosity (Y/N)	Porosity error (Y/N)	Particle Types	How	Size methods	Porosity methods	Data extraction method
Alldredge & Gotschalk, 1988[1]	Y	N	Y	N	Natural diatom & other marine snow	In situ SCUBA divers	Camera-based	Mass-based	Indirectly from Figure 2C
Logan & Alldredge, 1989[2]	Y	N	Y	Y	Natural diatom flocs	In situ SCUBA divers	Camera-based	Mass-based	Directly from Table 2
Lam & Bishop, 2007[3]	Y	Y	Y	N	Natural marine aggregates	In situ pump particles	UVP-based	Mass-based	Indirectly from Figure 14A & UVP PSD slopes
Ploug et al., 2008[4]	Y	Y	Y	Y	Various cultures, marine snow & fecal pellets	Lab roller tanks	Microscope-based	Mass-based	Directly from Table 1
Bach et al., 2016[5]	Y	Y	Y	N	Natural marine aggregates	In situ mesocosm	Camera-based	Mass-based	Personal communication
Ploug & Passow, 2007[6]	Y	Y	Y	Y	Diatom culture	Lab roller tanks	Microscope-based	Mass-based	Directly from Table 1
Engel et al., 2009[7]	Y	Y	Y	Y	*E. huxleyi* cultures	Lab roller tanks	Camera-based	Mass-based	Personal communication
Schmidt et al., 2014[8]	Y	Y	Y	Y	Diatom culture, coccoliths & foram tests	Lab roller tanks	Camera-based	Mass-based	Directly from text & indirectly from Figure 1B
Prairie et al., 2015[9]	Y	Y	Y	Y	Diatom cultures	Lab roller tanks	Microscope-based	Mass-based	Directly from Table 1 & 2
Iversen & Roberts, 2015[10]	Y	N	Y	N	<100 μm natural plankton	Lab roller tanks	Microscope-based	Mass-based	Personal communication
Laurenceau-Cornec et al., 2015[11]	Y	N	Y	N	Natural phytoplankton mixtures	Lab roller tanks	Camera-based	Mass-based	Personal communication
Laurenceau-Cornec et al., 2020[12]	Y	Y	Y	Y	Diatom cultures & zooplankton	Lab roller tanks	Microscope-based	Mass-based	Directly from Tables 2 & S1
Bach et al., 2019[13*]	Y	Y	Y	Y	Natural marine aggregates	In situ mesocosm	Camera-based	Optic-based	Directly from PANGAEA

*. The data from Bach et al. (2019) are not shown in Figure 2 in the main text, for it is optic-based and not calibrated with the mass-based method.

Table S2. *Properties of Size Bins in the Model*

Size bin	SSF			LSF		
	Size min (μm)	Size max (μm)	Center (μm)	Size min (μm)	Size max (μm)	Center (μm)
1	1.0	1.2	1.1	51.0	61.3	55.9
2	1.2	1.4	1.3	61.3	73.6	67.2
3	1.4	1.6	1.5	73.6	88.4	80.7
4	1.6	1.9	1.7	88.4	106.2	96.9
5	1.9	2.2	2.0	106.2	127.6	116.4
6	2.2	2.6	2.4	127.6	153.3	139.9
7	2.6	3.0	2.8	153.3	184.1	168.0
8	3.0	3.5	3.3	184.1	221.2	201.8
9	3.5	4.1	3.8	221.2	265.8	242.5
10	4.1	4.8	4.5	265.8	319.2	291.3
11	4.8	5.6	5.2	319.2	383.5	349.9
12	5.6	6.6	6.1	383.5	460.7	420.4
13	6.6	7.7	7.1	460.7	553.5	505.0
14	7.7	9.0	8.4	553.5	664.9	606.6
15	9.0	10.6	9.8	664.9	798.7	728.8
16	10.6	12.4	11.4	798.7	959.5	875.5
17	12.4	14.5	13.4	959.5	1152.7	1051.7
18	14.5	17.0	15.7	1152.7	1384.8	1263.4
19	17.0	19.8	18.3	1384.8	1663.5	1517.8
20	19.8	23.2	21.5	1663.5	1998.4	1823.3
21	23.2	27.2	25.1	1998.4	2400.7	2190.4
22	27.2	31.8	29.4	2400.7	2884.0	2631.3
23	31.8	37.2	34.4	2884.0	3464.6	3161.0
24	37.2	43.6	40.3	3464.6	4162.1	3797.4
25	43.6	51.0	47.1	4162.1	5000.0	4561.9